



Experimental Validation of a Nonextensive Scaling Law in Confined Granular Media

Gaël Combe,^{*} Vincent Richefeu, and Marta Stasiak

Université Grenoble Alpes, 3SR, F-38000 Grenoble, France and CNRS, 3SR, F-38000 Grenoble, France

Allbens P. F. Atman[†]

*Departamento de Física e Matemática, National Institute of Science and Technology for Complex Systems,
Centro Federal de Educação Tecnológica de Minas Gerais – CEFET-MG,
Avenida Amazonas 7675, 30510-000 Belo Horizonte-MG, Brazil*

(Received 28 July 2015; published 1 December 2015)

In this Letter, we address the relationship between the statistical fluctuations of grain displacements for a full quasistatic plane shear experiment, and the corresponding anomalous diffusion exponent α . We experimentally validate a particular case of the Tsallis-Bukman scaling law, $\alpha = 2/(3 - q)$, where q is obtained by fitting the probability density function (PDF) of the displacement fluctuations with a q -Gaussian distribution, and the diffusion exponent is measured independently during the experiment. Applying an original technique, we are able to evince a transition from an anomalous diffusion regime to a Brownian behavior as a function of the length of the strain window used to calculate the displacements of the grains. The outstanding conformity of fitting curves to a massive amount of experimental data shows a clear broadening of the fluctuation PDFs as the length of the strain window decreases, and an increment in the value of the diffusion exponent—anomalous diffusion. Regardless of the size of the strain window considered in the measurements, we show that the Tsallis-Bukman scaling law remains valid, which is the first experimental verification of this relationship for a classical system at different diffusion regimes. We also note that the spatial correlations show marked similarities to the turbulence in fluids, a promising indication that this type of analysis can be used to explore the origins of the macroscopic friction in confined granular materials.

DOI: [10.1103/PhysRevLett.115.238301](https://doi.org/10.1103/PhysRevLett.115.238301)

PACS numbers: 83.80.Fg, 45.70.Mg, 81.05.Rm

Turbulence is one of the most complex, but ubiquitous, phenomena observed in nature and it is related to the underlying mechanisms responsible for the micro-macro upscale causing wide-ranging effects on classical systems, like macroscopic friction in granular solids or turbulent flow regime in fluids [1–4]. The presence of multiple scales in time and space is an additional challenge to a comprehensive theoretical description, and a particular effort is made in the literature to perform experiments and simulations in order to validate the proposed theoretical descriptions, particularly Tsallis nonextensive (NE) statistical mechanics [5,6] as in the pioneering works of Sattin [7] and Arevalo *et al.* [8].

A paradigmatic work relating anomalous diffusion and turbulentlike behavior in confined granular media was presented by Radjai and Roux [4], using numerical simulations, and confirmed qualitatively by experiments by Combe and collaborators [9,10]. Radjai and Roux coined a new expression to characterize the analogies between fluctuations of particle velocities in quasistatic granular flows and the velocity fields observed in turbulent fluid flow in the high Reynolds number regime, the “granulence.” Most of the evidence of granulence is based on simulations using the discrete element method (DEM) but, unfortunately, there is a lack of quantitative

experimental verification recently, limiting the knowledge of the micromechanics of this system.

In the present work, we aim to fill this gap with the experimental validation of the results obtained by the DEM. Specifically, we seek to examine the findings revealed by Radjai and Roux [4] in a detailed fashion, extending the previous works [9,10] to explore quantitatively the relationship between the PDF of the velocity fluctuations and the diffusion features of the grains. We follow a detailed theoretical description for the anomalous diffusion in the presence of external driving [11,12]. Particularly, a relation between the q -Gaussian value from the PDF of fluctuations and the diffusion exponent was proposed, which is validated experimentally here for the first time for a large range of the control parameter, improving on previous works where this relation was tested only for a single point [13,14].

In this work, we advanced in the route opened by Radjai and Roux [4] with three basic goals: (i) *Explore the low inertial number limit.*—The inertial number I [15] measures the ratio between inertial and confining forces, from the quasistatic regime (small values) to the dynamic regime (large ones) [16]. We would like to check if the granulence features are still observed in a better established quasistatic situation, i.e., the experimental one which involves inertial numbers around 4 orders of magnitude smaller than that

currently reported in simulations [17]. (ii) *Pinpoint the origins of the macroscopic friction.*—We take advantage of the really quasistatic nature of the experimental data to explore the origins of the underlying mechanisms of granulence. Here, unlike fluid flow, the rigid particles cannot fly freely since the motion of each particle is hampered by the presence of the other particles, and depends on the motion of its neighbors. This makes the straining in part controlled by geometric exclusions at the particle scale, preventing the development of a uniform straining in a sustainable way. As shown in Ref. [9], at the limit of large strain windows, it is possible to observe turbulentlike vortexes in the fluctuation field, which turn out to be associated with the energy dissipation and macroscopic friction [18–20]. (iii) *Evince the nonextensive nature of the displacement fluctuations.*—In order to quantitatively analyze the data, the Tsallis NE statistical mechanics approach was used. In this context, the PDF of displacement fluctuations is not expected to follow the normal Gaussian distribution, as in the case of classical Maxwell-Boltzmann distribution in thermodynamics. In granular systems under loading, the force chains engaged along the entire system are a clear evidence of long-range interactions [21]. These chains connect the microscopic contact forces with the global resistance to external forces, as in, for example, shear [22]. Thus, it is natural to associate the emergence of these force chains at mesoscopic scales with the departure from the classical Boltzmann-Gibbs (BG) statistics in these systems.

In the experiment, we have foreseen the possibility to quantify the degree of nonextensivity using the q -Gaussian fit of the PDF obtained experimentally [9]. The striking accordance observed on the fitted curves, and the dependence observed of q as a function of the strain window used to calculate the fluctuations, according to the reasoning presented here, corroborates the application of the NE statistical mechanics on these systems, opening an alternative approach to treat these systems quantitatively. Besides, by measuring the diffusion of the particles along the complete shear test, with different strain windows, we are able to associate the q value measured from the fluctuation PDFs with the diffusion exponent α . This is a particular case of the Tsallis-Bukman scaling law [11] (corresponding to the case $\mu = 1$ and $q = 2 - \nu$ in the original paper of Tsallis Bukman, which preserves the norm, the physically consistent case),

$$\alpha = \frac{2}{3 - q}, \quad (1)$$

which can be obtained from the *porous media equation* [12], a generalization of the classical diffusion equation where the linear dependence between the variance and time is no longer observed [23]:

$$\frac{\partial p(x, t)}{\partial t} = D_q \frac{\partial^2 [p(x, t)]^{2-q}}{\partial x^2}. \quad (2)$$

For a Dirac delta initial condition, the solution reads as

$$p_q(x, t) = \frac{1}{\sqrt{\pi A_q}} e_q^{-(x^2/A_q)} \equiv \frac{1}{\sqrt{\pi A_q}} \left[1 - (1 - q) \frac{x^2}{A_q} \right]^{[1/(1-q)]}, \quad (3)$$

where $e_q(x)$ is called the q exponential, and A_q is a constant that depends on q and the Gamma function [6,12].

Equation (3) is known as the q Gaussian distribution, and was used to fit the PDF of displacement fluctuations obtained experimentally. Figure 2 shows the results for the PDF of fluctuations and the corresponding fit function at two extremal values of $\Delta\gamma$ considered in the image analysis.

In the case of anomalous diffusion, it is shown that the variance follows a power law with time:

$$\langle x^2 \rangle \propto t^\alpha \equiv \langle x^2 \rangle \propto t^{[2/(3-q)]}, \quad (4)$$

where α is the diffusion exponent equivalently expressed as a function of q by using Eq. (1). Note that, in Eqs. (2)–(4), x stands for a fluctuation of displacement as we will see below. It is interesting to observe two special cases: when $q = 1$, the variance is proportional to time, which corresponds to the normal diffusion behavior; when $q = 2$, the ballistic diffusion limit is reached. At intermediate values, we get large distributions with marked tails. The variance, calculated as the time integral of p_q , diverges for $q > 5/3$, and converges otherwise. Thus, if several independent convolutions are applied, p_q approaches a Gaussian distribution if $q < 5/3$, and it approaches a Lévy distribution for $q > 5/3$ [6].

We performed quasistatic simple shear tests [24] with the $1\gamma 2\varepsilon$ apparatus, which is fully described in Refs. [25,26]. The granular packing is made of pilings of cylindrical rods that mimics a 2D granular material enclosed by a rectangular frame, with initial dimensions of 0.56×0.47 m. Then, the vertical sides of this rectangular parallelogram are shortened or elongated to apply a constant normal stress in the vertical direction, $\sigma_n = 50$ kPa. These two vertical sides are tilted up to $\gamma = 15^\circ$ while the two other sides are kept horizontal with a constant length; see Fig. 1. The packing was made of 5471 wooden rollers (6 cm long) with ten different diameters ranging from 3 to 30 mm, approaching a uniform distribution. To ensure a quasistatic transformation of the sample, it is sheared very slowly—the corresponding shear rate $\dot{\gamma}$ is $4.5 \times 10^{-5} \text{ s}^{-1}$. This ensures a very small inertial number [16] ($I = 10^{-9}$) when compared to what is applied in DEM simulations (10^{-3} to 10^{-5} in the best cases) [17,27]. During the test, kinematics of grains are measured by means of digital image correlation (DIC) [28,29] from 80 Mpixel digital images of the sample where rollers look like disks, Fig. 1. A specific DIC computer program was developed to track rollers here assumed as rigid bodies [10], which allowed a subpixel kinematics measurement to track grains with an error of ± 0.05 pixels [30].

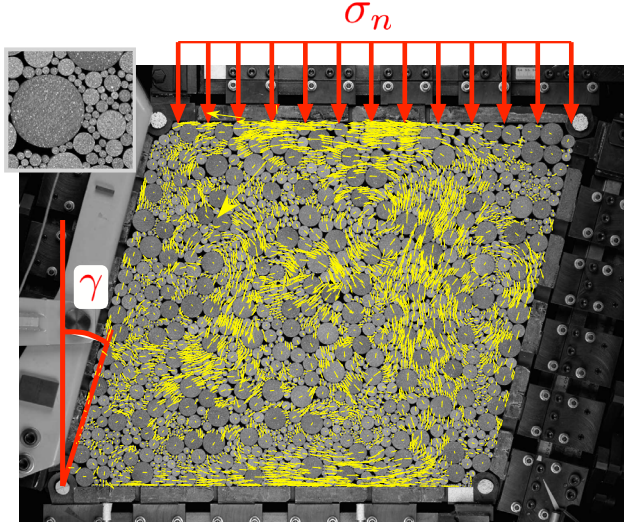


FIG. 1 (color online). The fluctuating part of the rod displacement $\mathbf{v}(\gamma, \Delta\gamma)$ overplotted on the corresponding digital image, obtained from DIC. $\gamma = \Delta\gamma = 0.1$. Inset: a detailed view of the speckled rods. γ and σ_n are the shear angle and the vertical stress imposed, respectively. The shear strength is measured all along the shear test.

At the macroscopic level (sample scale), the stress-strain curve measured during the shear test exhibited hardening up to $\gamma \approx 0.06$ followed by softening until the end of the test (curve shown in Ref. [10] as well as several other mechanical properties like the peak stress ratio, macroscopic friction angle, etc.). Pictures were shot every $\delta t = 5$ s throughout the test, corresponding to a shear strain increment $\Delta\gamma \equiv \delta t \dot{\gamma} \approx 2.4 \times 10^{-4}$ between each shot. To assess the displacement fluctuations, we consider two displacements of each particle during a shear increment $\Delta\gamma$. The first is the actual displacement $\delta\mathbf{r}(\gamma, \Delta\gamma)$ from γ to $\gamma + \Delta\gamma$. The second displacement, $\delta\mathbf{r}^*(\gamma, \Delta\gamma)$, is fictitious and corresponds to an affine motion resulting from a homogeneous straining at γ and during the shear-increment $\Delta\gamma$. It is assessed from the motion of the four rigid sides of the apparatus $1\gamma 2\epsilon$. With these definitions, the fluctuating part of the displacement is the difference between the actual and affine displacements. Thus, the normalized displacement fluctuation $\mathbf{v}(\gamma, \Delta\gamma)$ is defined by

$$\mathbf{v}(\gamma, \Delta\gamma) = \frac{[\delta\mathbf{r}(\gamma, \Delta\gamma) - \delta\mathbf{r}^*(\gamma, \Delta\gamma)]/d}{\Delta\gamma}, \quad (5)$$

where d is the mean diameter of the rollers. One may notice that the normalized fluctuations can be interpreted as a local strain (grain scale, numerator) compared to the global strain (sample scale, denominator).

A displacement fluctuation field \mathbf{v} is plotted in Fig. 1 for a given shear increment. One can notice an organization in structures like vortices, reminiscent of those observed in the turbulence phenomena in fluids. These structures found their origins in the rearrangement mechanism of the grains,

since the elements interfere with each other in their affine movement. This is, in other words, the deviation from the affine field due to steric exclusion forming patterns observed with discrete element modeling [15,31,32] and more rarely in experiments [19]. Their dynamics depend both on γ and $\Delta\gamma$, evolving gently under shear when $\Delta\gamma$ is large (> 0.04) and very rapidly for small values ($\Delta\gamma \approx 2.4 \times 10^{-4}$). The characteristic lengths depend strongly on $\Delta\gamma$, with vortices of a few tenths of mean grain diameter for large values of $\Delta\gamma$, and, to the contrary, for small values of $\Delta\gamma$ these structures are not well defined, and long-range correlations are observed [10].

The PDFs of the horizontal component magnitude of normalized displacement fluctuations are shown in Fig. 2 for two different increments of shear strain: $\Delta\gamma = 7.3 \times 10^{-4}$ and $\Delta\gamma = 10^{-1}$. We observe a broadening of the PDF from a nearly Gaussian distribution (for large $\Delta\gamma$) to a wider distribution (for small $\Delta\gamma$).

The dependence of the q exponent with the strain window used to calculate the fluctuations is shown in Fig. 3 for experimental and simulation data. Two remarkable features can be observed in this plot. First, in the limit of a large strain window, when the abscissa goes to zero, $q \rightarrow 1$, indicating the limit when normal diffusion and the BG statistics are satisfied. Note that it is possible to test larger values of $\Delta\gamma$ in DEM simulations which confirm the limit $q \rightarrow 1$ (data shown in the inset of Fig. 3). This is exactly what we expect for this limit, once the particles typically experience several collisions and rearrangements, approaching to the molecular chaos hypothesis.

Second, at the other limit, for a vanishing strain window, the q value attains a plateau, with $q \sim 3/2$. This observation can be interpreted as a sign of the long-range correlations imposed by the force chains at this short time scale. Once the value measured for q in this limit is lower than $5/3$, one can expect that for large strain windows a Gaussian

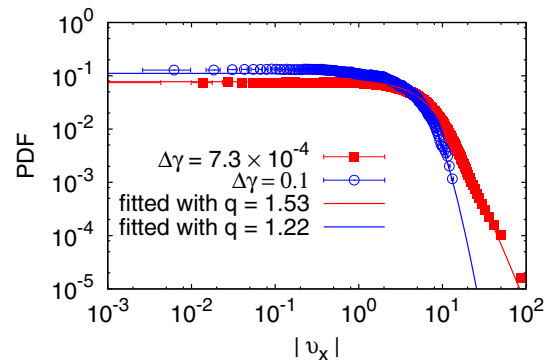


FIG. 2 (color online). Probability density functions of the horizontal components of the fluctuating displacements tracked during two different increments of shear strain ($\Delta\gamma = 7.3 \times 10^{-4}$ and $\Delta\gamma = 10^{-1}$). The scatters correspond to experimental data, and the solid lines correspond to regressions of function p_q [Eq. (3)] that allow for assessment of the q values.

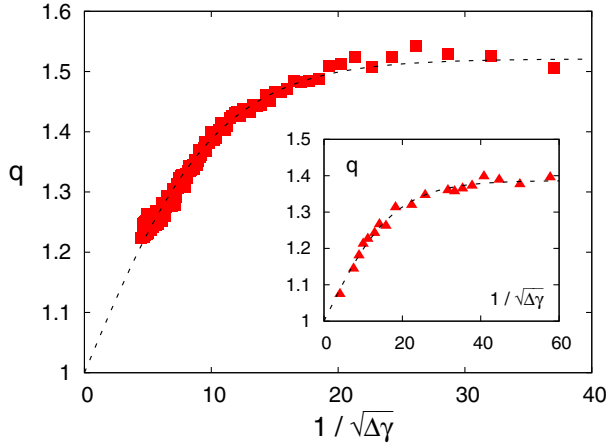


FIG. 3 (color online). Evolution of the measured q value as a function of the squared inverse of the strain increment for the experiments and simulations. The dashed line corresponds to a regression using the function $q(1/\sqrt{\Delta\gamma}) = 1 + a \tanh(b/\sqrt{\Delta\gamma})$, with $a = 0.521$, $b = 0.096$. Inset: the same plot for data from a DEM simulation that highlights the limit $q = 1$ when $\Delta\gamma \rightarrow \infty$. The fitted parameters for simulations were $a = 0.387$, $b = 0.057$.

distribution would be recovered, since it corresponds to successive independent convolutions of q -Gaussian distributions.

These features were observed both in experiments and simulations, no matter the differences among the systems (periodic boundaries in horizontal direction in simulations, different number of particles, and inertial numbers, etc.), proving the robustness of the result.

Analyzing the results as a whole, we can sketch a phenomenological scenario to explain the observations: in the limit of large $\Delta\gamma$, we observe a tendency to agree with the BG statistics, with $q \rightarrow 1$. This limit corresponding to the transition from meso- to macroscopic scales, and the formation of vortices in the spatial distribution of fluctuations, as shown in Fig. 1. These vortices, with few grain diameters in size, interact with each other to dissipate the excess energy due to external loading, in analogy with the role of vortices in turbulent flow [4]. The broadening of the distribution of displacements fluctuations is usually attributed to the energy cascade from larger to lower scales, that is, from large vortices to the small ones [4]. More similarities between turbulence in fluids and granulence are explored in Refs. [4,9].

On the other hand, we have $q \approx 3/2$ for the vanishing strain-window's limit, $\Delta\gamma \rightarrow 0$. This result indicates the presence of long-range interactions and anomalous diffusion. Considering the absence of spatial structures on the fluctuation field, it is clear that this limit is dominated by the force chain dynamics. Force chains can span all along the system, but are very fragile, implying short lifetimes. The displacement of grains belonging to a force chain is strong correlated spatially, but this correlation is not verified for large temporal scales.

Thus, we can conclude that the window used to measure the PDF particle displacement fluctuations in the system plays a crucial role in the statistics that will be obtained. Basically, it is possible to explore the micro-macro transition on the PDF distributions, from a correlated regime dominated by the force chains to a frictional stochastic one, dominated by spatial vortex interactions. This conclusion has a striking implication for any analysis concerning the measuring of displacement fluctuations, since it unveils how the observation procedure can alter the conclusions even in a relatively simple diffusion experiment. Similar behavior could be observed in other systems which display long-range spatial correlations, externally driven with different frequencies, quite a common situation.

To quantify the diffusion of the grains along the complete shear test we simply computed the average displacement of each grain as a function of time (shear increment γ), but with different sampling frequencies determined by the strain-window $\Delta\gamma$. Following the reasoning presented above, and Eq. (4), we should expect two extreme regimes

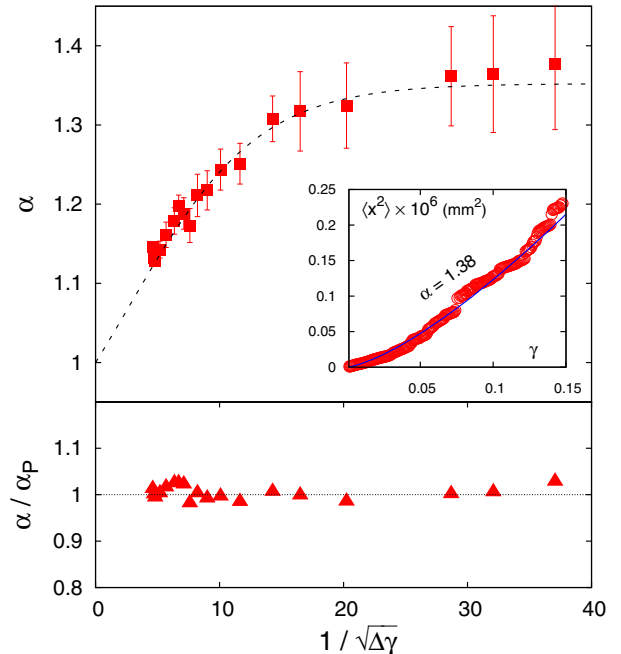


FIG. 4 (color online). Verification of the Tsallis-Bukman scaling law for different regimes of diffusion. (Top) Evolution of the measured diffusion exponent α as a function of $1/\sqrt{\Delta\gamma}$; the dashed line is a direct application of the scaling law from the fit of the values shown in Fig. (3), $\alpha(1/\sqrt{\Delta\gamma}) = 2/[3 - q(1/\sqrt{\Delta\gamma})]$. (Inset) a typical diffusion curve showing the mean square displacement fluctuations $\langle x^2 \rangle$ in a function of the shear strain γ ; it allows the assessment of the diffusion exponent α for each strain window tested. In the case shown, it corresponds to the smallest strain window, the rightmost point in the curve at the main panel. Note that for a constant strain rate, γ is proportional to time. (Bottom) Measure of the deviation of the data relative to the scaling law prediction, as a function of $1/\sqrt{\Delta\gamma}$, showing an agreement on the order of $\pm 2\%$.

for the diffusion, analogously to that observed for the q value: an anomalous diffusion regime with $\alpha \sim 4/3$ for the vanishing strain window, and an asymptotic regime with $\alpha \rightarrow 1$ for large shear increments. This is indeed what we can observe in Fig. 4, where we have verified the Tsallis-Bukman scaling law [Eq. (1)]. It is important to stress that the dashed line in Fig. 4 is *not* a direct fit, but rather the curve obtained in Fig. 3 using the Tsallis-Bukman scaling law. To our knowledge, it is the first time that this relation is verified for different regimes of diffusion. This striking result reinforces the use of the Tsallis NE statistical mechanics to describe strongly correlated systems, as in the case of confined granular material under shearing.

We are in debt to Constantino Tsallis for the fruitful discussions, suggestions, and kind reading of the manuscript. We thank Philippe Claudin and Edward Andò for the kind reading of the manuscript and suggestions. We are grateful to Jean-Benoît Toni for his valuable work to upgrade the electronic part of $1\gamma 2\epsilon$ apparatus. A special thanks to François Bonnel without who we would not have the chance to shoot with the Phase One IQ180 camera (80 MPixels). A. P. F. A. thanks the Brazilian funding agencies FAPEMIG, CNPq, and CAPES, and CEFET-MG for financial support. The Laboratoire 3SR is part of the LabEx Tec 21 (Investissements d’Avenir, Grant Agreement No. ANR-11-LABX-0030).

*gael.combe@3sr-grenoble.fr

†atman@dppg.cefetmg.br

- [1] T. Nguyen, G. Combe, D. Caillerie, and J. Desrues, *Acta Geophys.* **62**, 1109 (2014).
- [2] D. C. Wilcox, *AIAA J.* **26**, 1311 (1988).
- [3] T. Hou, X. Hu, and F. Hussain, *J. Comput. Phys.* **232**, 383 (2013).
- [4] F. Radjai and S. Roux, *Phys. Rev. Lett.* **89**, 064302 (2002).
- [5] C. Tsallis, *J. Stat. Phys.* **52**, 479 (1988).
- [6] C. Tsallis, *Introduction to Nonextensive Statistical Mechanics: Approaching a Complex World*, 1st ed. (Springer, New York, 2009).
- [7] F. Sattin, *J. Phys. A* **36**, 1583 (2003).
- [8] R. Arevalo, A. Garcimartin, and D. Maza, *Eur. Phys. J. E* **23**, 191 (2007).
- [9] G. Combe, V. Richefeu, G. Viggiani, S. A. Hall, A. Tengattini, and A. P. F. Atman, *AIP Conf. Proc.* **1542**, 453 (2013).
- [10] V. Richefeu, G. Combe, and C. Viggiani, *Géotechnique Letters* **2**, 113 (2012).
- [11] C. Tsallis and D. J. Bukman, *Phys. Rev. E* **54**, R2197 (1996).
- [12] A. R. Plastino and A. Plastino, *Physica (Amsterdam)* **222A**, 347 (1995).
- [13] A. Upadhyayaa, J.-P. Rieu, J. A. Glazier, and Y. Sawadac, *Physica (Amsterdam)* **293A**, 549 (2001).
- [14] K. E. Daniels, C. Beck, and E. Bodenschatz, *Physica (Amsterdam)* **193D**, 208 (2004).
- [15] J.-N. Roux and G. Combe, *Proceedings of the 16th ASCE Engineering Mechanics Conference* (ASCE, Reston, VA, 2003), Vol. 48, p. 56.
- [16] G. MiDi, *Eur. Phys. J. E* **14**, 341 (2004).
- [17] F. Radjai and F. Dubois, *Discrete-Element Modeling of Granular Materials* (Wiley-Iste, New York, 2011).
- [18] P. G. Rognon, T. Miller, B. Metzger, and I. Einav, *J. Fluid Mech.* **764**, 171 (2015).
- [19] T. Miller, P. Rognon, B. Metzger, and I. Einav, *Phys. Rev. Lett.* **111**, 058002 (2013).
- [20] See Supplemental Material at <http://link.aps.org/supplemental/10.1103/PhysRevLett.115.238301> for movie animations of the temporal evolution of the displacement fields at two extremal values of the strain window.
- [21] T. S. Majmudar and R. P. Behringer, *Nature (London)* **435**, 1079 (2005).
- [22] N. Estrada, A. Taboada, and F. Radjai, *Phys. Rev. E* **78**, 021301 (2008).
- [23] T. Pöschel and S. Luding, *Granular Gases*, Lecture Notes in Physics (Springer, New York, 2001).
- [24] <https://youtu.be/ZAP5BCGgZys>.
- [25] H. Joer, J. Lanier, J. Desrues, and E. Flavigny, *Geotech. Test. J.* **15**, 129 (1992).
- [26] F. Calvetti, G. Combe, and J. Lanier, *Mech. Cohes.-Fric. Mater* **2**, 121 (1997).
- [27] J. N. Roux and G. Combe, *AIP Conf. Proc.* **1227**, 260 (2010).
- [28] Z. He, M. Sutton, W. Ranson, and W. Peters, *Exp. Mech.* **24**, 117 (1984).
- [29] T. Chu, W. Ranson, and M. Sutton, *Exp. Mech.* **25**, 232 (1985).
- [30] G. Combe and V. Richefeu, *AIP Conf. Proc.* **1542**, 461 (2013).
- [31] M. R. Kuhn, *Mech. Mater.* **31**, 407 (1999).
- [32] G. Combe and J. Roux, *C.R. Phys.* **3**, 131 (2002).